

# Enrichment of Helium by Asymmetric Hollow-Fiber Membrane of Cellulose Triacetate

H. KUMAZAWA,<sup>1,\*</sup> E. SADA,<sup>1</sup> K. NAKATA,<sup>1</sup> N. KAWASHIMA,<sup>2</sup> S. KATAOKA,<sup>2</sup> and K. TADA<sup>2</sup>

<sup>1</sup>Department of Chemical Engineering, Kyoto University, Kyoto 606-01, Japan;

<sup>2</sup>Kawasaki Heavy Industries, Ltd., Kobe 650-91, Japan

## SYNOPSIS

The permeation behavior of pure He and separation characteristics of He-air mixtures were examined using asymmetric hollow-fiber-type membrane modules of cellulose triacetate. The module was operated in a feed-outside mode. In permeation of pure He, the permeation rate coefficients slightly increased with increasing upstream pressure, and they agreed fairly well with those calculated on the basis of the assumption that the permeate flow inside the fiber is governed by the Hagen-Poiseuille equation. In the single-stage hollow-fiber module used, the molar fraction of He in the permeate stream was increased to 0.99 and 0.999 at the stage cuts of lower than 0.3 when the molar fraction in the feed stream was 0.90 and 0.99, respectively. The molar fractions of He in the permeate stream were numerically evaluated for various combinations of operating conditions in terms of a countercurrent plug flow model. © 1994 John Wiley & Sons, Inc.

## INTRODUCTION

Membrane gas-separation systems practically use asymmetric membranes in the form of hollow fibers, because high permeation flux and rate as well as high permselectivity can be achieved at the same time. The performance of such membranes strongly depends on the feed-permeate flow pattern, i.e., on the countercurrent, cocurrent, or cross-flow.<sup>1,2</sup> Furthermore, for the high-flux asymmetric membrane, where the permeate flows inside the fiber, the permeate pressure buildup is apt to be excessive,<sup>3</sup> or the significant feed pressure drop emerges if the feed flows inside the fiber. To understand the separation behavior of such membranes, these items should be taken into account.

The present study was undertaken to obtain fundamental data and findings to achieve the high degree of purification of helium from helium-air mixtures by membrane separation. The hollow-fiber module of asymmetric cellulose triacetate was employed as the helium-separation device. The permeation behavior and separation characteristics

were tested specifically in the high concentration regime, where the composition of helium in the feed was greater than 90 vol %.

## EXPERIMENTAL

Helium enrichment runs were carried out using a hollow-fiber-type membrane permeator. The unit consists of a bundle of asymmetric hollow fibers of cellulose triacetate. The skin layer of the asymmetric membrane is formed on the outer surface of the hollow fiber. The schematic diagram of the experimental apparatus is shown in Figure 1. The feed-outside operation mode has been employed. The feed gas is on the skin side of the asymmetric membrane. Four kinds of hollow-fiber module with different dimensions have been used in the permeation experiments. These hollow fibers of cellulose triacetate were kindly provided by Toyobo Co., Japan. The geometric properties of the modules are listed in Table I.

First, pure He, O<sub>2</sub>, and N<sub>2</sub> were used as a penetrant gas, and permeation characteristics of the hollow-fiber membrane modules were measured. Second, mixtures of He and air containing 90.0 and 99.0% He were permeated, and separation behavior

\* To whom correspondence should be addressed.

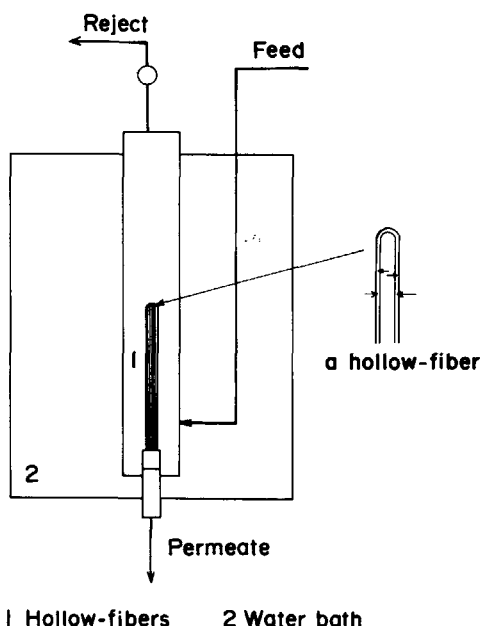


Figure 1 Schematic diagram of experimental apparatus.

was investigated. The concentrations of  $N_2$  and  $O_2$  in the permeate stream were determined using a gas chromatograph with a 2.5 m-long column packed with molecular sieve 13X. The column temperature was held at  $60^\circ\text{C}$ , and helium was used as the carrier gas.

For the sake of comparison with the permeation behavior of asymmetric hollow-fiber-type membranes, permeation runs for pure He and  $O_2$  were performed using a flat homogeneous dense membrane of cellulose triacetate. The permeation cell used was the same one as used in our previous work.<sup>4</sup> The cross section (i.e., permeation area) of the cell was  $19.6\text{ cm}^2$ . The steady-state permeation rate was measured by the variable volume method. Cellulose triacetate membrane samples (FT 0.05) were kindly supplied by Fuji Film Co., Japan. The nominal thickness of the membrane was  $50\ \mu\text{m}$ . All perme-

Table I Dimensions of Membrane Modules

	Sample No.			
	11	13	21	24
$D_o$ (mm)	0.148	0.188	0.191	0.191
$D_i$ (mm)	0.056	0.097	0.088	0.088
$L_i$ (cm)	22	16	87	21
$N_i$	180	240	240	240
$A_i$ ( $\text{cm}^2$ )	184	227	1253	317

ation and separation experiments were carried out at  $20$  and  $30^\circ\text{C}$  and with upstream pressures of up to  $2.4\text{ MPa}$ .

## RESULTS AND DISCUSSION

### Permeation of Pure Gas

Measured steady-state permeation rates for pure gases were converted to the permeation rate coefficients defined by

$$\kappa = \bar{P}/\delta = J_s/(p_2 - p_1) \quad (1)$$

where  $\bar{P}$  refers to the mean permeability coefficient, and  $\delta$ , to the thickness of the skin layer of the asymmetric hollow-fiber membrane. The permeation rate coefficients for He,  $O_2$ , and  $N_2$  in asymmetric hollow-fiber modules 21 and 24 were plotted against the difference between pressures of feed and permeate sides in Figures 2 and 3, respectively. The coefficients for  $O_2$  and  $N_2$  are shown to be independent of the pressure difference, whereas those for He def-

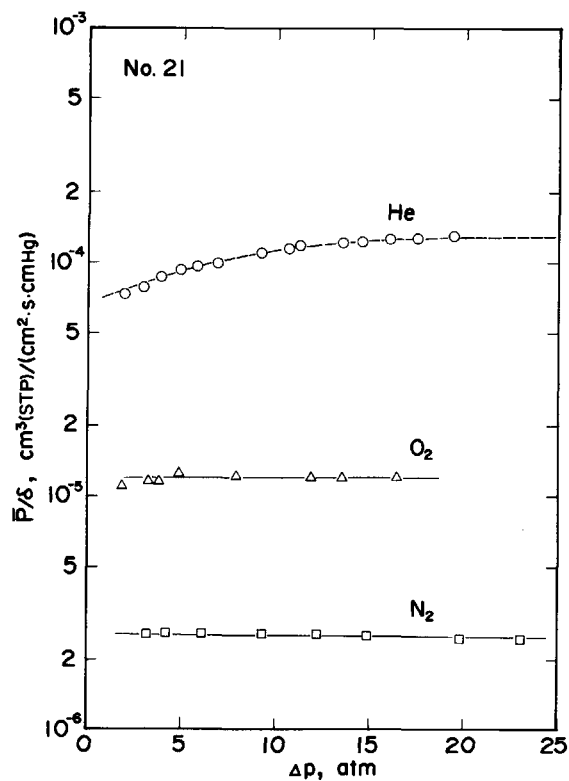
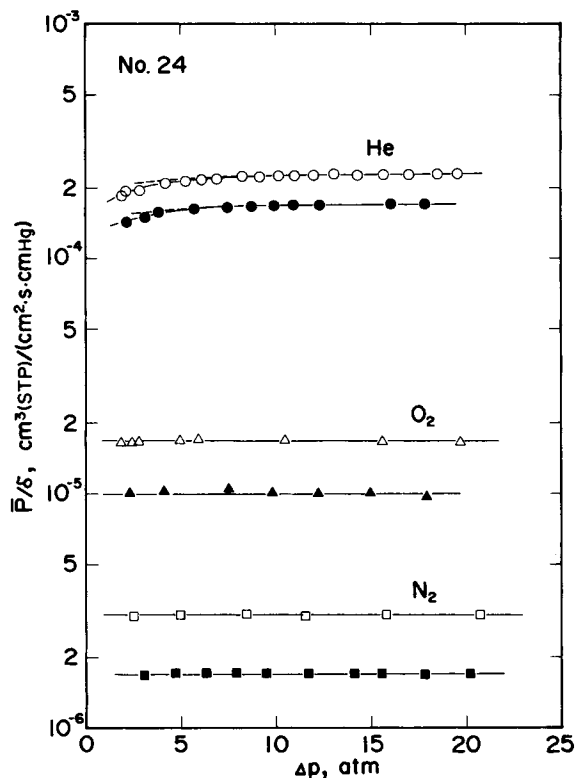


Figure 2 Permeation rate coefficients as a function of pressure difference for He,  $O_2$ , and  $N_2$  in asymmetric hollow fibers of cellulose triacetate (sample 21) at  $30^\circ\text{C}$ .



**Figure 3** Permeation rate coefficients as a function of pressure difference for He, O<sub>2</sub>, and N<sub>2</sub> in asymmetric hollow fibers of cellulose triacetate (sample 24) at 20°C (full keys) and 30°C (open keys).

initially depend on the pressure difference, i.e., the increase with an increase in the pressure difference up to 20 and 5 atm for modules 21 and 24, respectively. The values of the mean permeation rate coefficient for He,  $(\bar{P}/\delta)_{\text{He}}$ , at  $p_2 = 10$  atm and the values of the separation factor defined as the ratio of  $(\bar{P}/\delta)_{\text{He}}$  at  $p_2 = 10$  atm to  $(P/\delta)_{\text{O}_2}$  in four membrane modules are listed in Table II. The separation factors

range from 9.5 to 15.2. To investigate whether such a pressure dependence for He is caused by the membrane material (cellulose triacetate), mean permeability coefficients for He through a flat membrane of cellulose triacetate were measured. The mean permeability coefficients were plotted against the pressure difference in Figure 4. They are found to be independent of the pressure difference. In Table II, the value of the ideal separation factor of this homogeneous membrane defined as the ratio of permeability for He to that for O<sub>2</sub> is listed together with the value of permeability for He. The ideal separation factor is compared to separation factors of asymmetric hollow-fiber membrane modules.

The pressure dependence of the permeation rate coefficient for He in the asymmetric hollow-fiber modules is deduced to be caused by the permeate pressure buildup inside the hollow fiber. Then, the permeation rate coefficient will be theoretically derived on the basis of the assumption that the permeate flow inside the fiber is governed by the Hagen-Poiseuille equation.

The permeation rate per a hollow fiber across a differential length  $dl$ , depicted in Figure 5, can be expressed as

$$\frac{dV}{dl} = \pi D_0 \left( \frac{P}{\delta} \right) (p_2 - p) \quad (2)$$

where  $P$  refers to the intrinsic permeability coefficient of the skin layer in the asymmetric hollow-fiber membrane. The membrane permeate pressure drop inside the hollow fiber is described by use of the Hagen-Poiseuille equation, viz.

$$\frac{dp}{dl} = - \frac{128RT\mu V}{\pi D_i^4 p} \quad (3)$$

**Table II** Permeabilities for He and Separation Factors for He Relative to O<sub>2</sub> in Hollow-Fiber Membrane Modules and a Flat Membrane at 30°C

	Hollow Fibers				Flat Membrane FT0.05
	No. 11	No. 13	No. 21	No. 24	
$(\bar{P}/\delta)_{\text{He}} \times 10^4$ <sup>a</sup>	1.08	1.58	1.09	2.23	—
$\bar{P}_{\text{He}} \times 10^9$ <sup>b</sup>	—	—	—	—	1.06
$\alpha'$ <sup>c</sup>	10.2	15.2	9.48	13.3	15.6
$(P/\delta)_{\text{He}} \times 10^4$	1.50	1.65	1.94	2.52	—
$\alpha$ <sup>d</sup>	14.2	15.9	16.9	15.0	15.6

<sup>a</sup> Values at  $p_2 = 10$  atm,  $[\text{cm}^3(\text{STP})/(\text{cm}^2 \text{ s cmHg})]$ .

<sup>b</sup>  $[\text{cm}^3(\text{STP}) \text{ cm}/(\text{cm}^2 \text{ s cmHg})]$ .

<sup>c</sup>  $\alpha' = (\bar{P}_{\text{He}} \text{ at } p_2 = 10 \text{ atm})/P_{\text{O}_2}$ .

<sup>d</sup>  $\alpha = P_{\text{He}}/P_{\text{O}_2}$ .

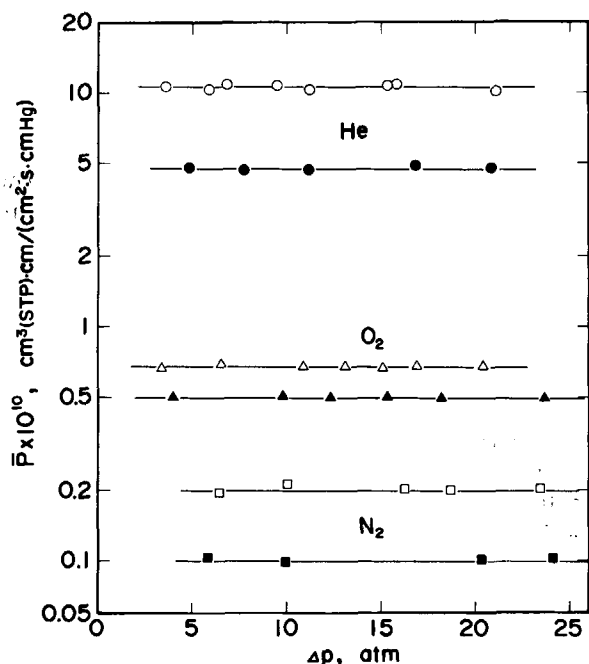


**Figure 4** Permeability coefficients as a function of pressure difference for He, O<sub>2</sub>, and N<sub>2</sub> in a flat homogeneous membrane of cellulose triacetate at 20°C (full keys) and 30°C (open keys).

On referring to Figure 5, the boundary conditions for the differential eqs. (2) and (3) are written as follows:

$$\text{at } l = 0, \quad p = p_0 \quad (4)$$

$$\text{at } l = L_t, \quad p = p_1 \quad (5)$$

Let the permeate flow rate at  $l = L_t$  be replaced with  $V_t$ , and then the mean permeability coefficient for the whole hollow fiber can be calculated as

$$\frac{\bar{P}}{\delta} = \frac{V_t}{\pi D_0 L_t (p_2 - p_1)} \quad (6)$$

Division of eq. (2) by eq. (3) leads to

$$\frac{dV}{dp} = - \frac{\pi^2 D_0 D_i^4 (P/\delta) (p_2 - p) p}{128 RT \mu V} \quad (7)$$

Integration of eq. (7) with respect to  $p$  from  $p_0$  to  $p_1$  yields  $V_t$  at  $p = p_1$  (i.e.,  $l = L_t$ ). The total length of the hollow fiber then can be calculated from integration of eq. (3) with respect to  $p$  from  $p_0$  to  $p_1$ , viz.

$$L_t = \int_0^{L_t} dl = - \int_{p_0}^{p_1} \frac{\pi D_i^4 p dp}{128 RT \mu V} \quad (8)$$

Accordingly, the permeation rate coefficient can be calculated by eq. (6).

Computational results of the mean permeation rate coefficients of He for samples 21 and 24 were shown as broken curves in Figures 2 and 3. The values of the intrinsic permeation rate coefficient ( $P/\delta$ ) used in the computation are listed in Table II. Ideal separation factors defined as  $(P/\delta)_{\text{He}}/(P/\delta)_{\text{O}_2}$  were calculated and are listed also in the same table. The ideal separation factors calculated thus are not varied so much module to module and are close to the ideal separation factor of a homogeneous membrane, whereas the separation factors defined as the ratio of  $(\bar{P}/\delta)_{\text{He}}$  at 10 atm to  $(P/\delta)_{\text{O}_2}$  range from 9.5 to 15.2. The agreement of broken curves with experimental points is shown to be rather good. The length of hollow fibers in the module of sample 21 is as great as 87 cm, and a considerably great pressure dependence of the mean permeation rate coefficient is exhibited. Specifically, the pressure dependence of the coefficient for this module is simulated well. The pressure at the closed end of the hollow fiber ( $p_0$ ) can also be evaluated along with the mean permeation rate coefficient. Figure 6 shows calculated relationships between  $p_0$  and pressure in the feed stream ( $p_1$ ) for four permeator modules. The permeate pressure buildup inside the hollow fiber is found to be greater than expected from the observed pressure dependence of the mean permeation rate coefficient. Specifically, for samples 11 and 21, which possess a finer diameter of the hollow fiber and longer hollow fibers, respectively, the pressure buildup inside the fiber is very great.

### Enrichment of Helium

Typical examples of the experimental results on separation of He-air mixtures containing 90 and 99 vol % He are shown as plots of concentration of He in permeate stream ( $y_p$ ) vs. stage cut ( $\theta$ ) in Figures 7 and 8. The stage cut here is defined as the fraction of the feed that is allowed to permeate through the membrane. In these figures,  $\gamma$  is an operating vari-

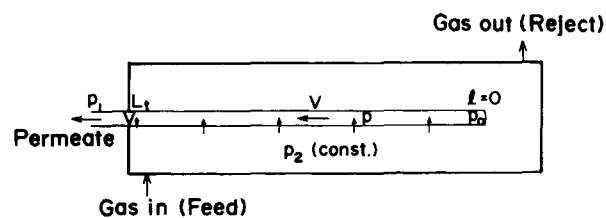


**Figure 5** Membrane permeator configuration.

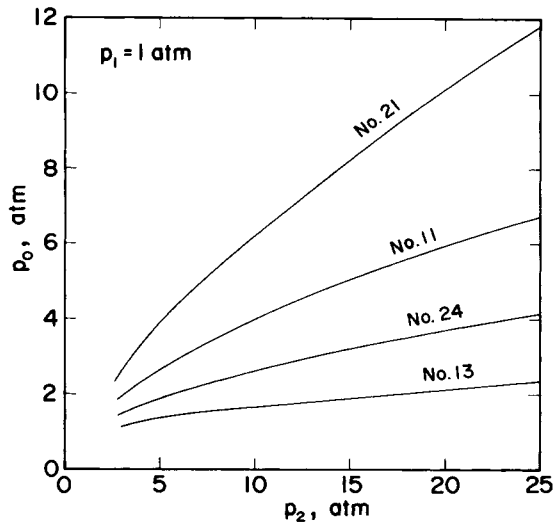


**Figure 6** Permeate-side pressure at the closed end of the hollow fiber as a function of feed-side pressure for different hollow-fiber membrane modules.

able defined as the ratio of downstream pressure (1 atm) to upstream pressure ( $p_2$ ). It is found that the concentration of He in the permeate stream only slightly increases with increasing upstream pressure. These figures show that at the stage cuts of lower than 0.3 the molar fraction of He in the permeate stream is increased to 0.99 and 0.999 when the molar fraction in the feed stream is 0.9 and 0.99, respectively; i.e., one order of magnitude of He enrichment can be achieved in a single stage of such a hollow-fiber-type membrane module.

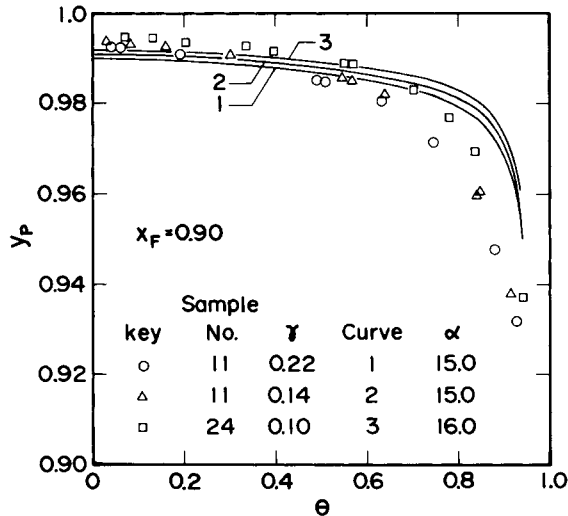


**Figure 7** Relationship between molar fraction of He in the permeate stream and stage cut at a molar fraction of He of 0.90 in the feed stream. Solid curves refer to calculated ones.

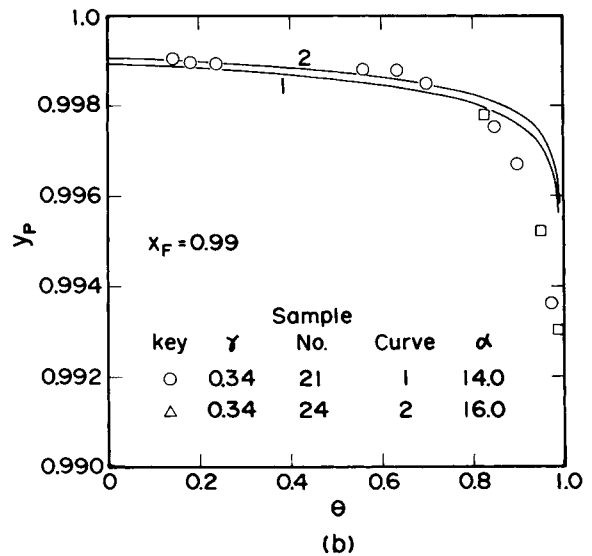
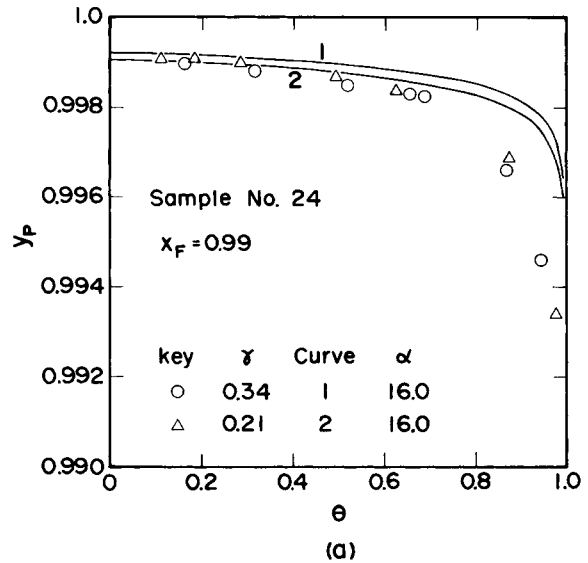


**Figure 8** Relationship between molar fraction of He in the permeate stream and stage cut at a molar fraction of He of 0.99 in the feed stream. Solid curves refer to calculated ones.

The concentration of He in the permeate stream was numerically evaluated from typical hollow-fiber-type membrane modules by a simple countercurrent plug flow model.<sup>1</sup> The calculation method for this model has been reported in the literature.<sup>1</sup> The model is based on the premise that the high- and low-pressure gas streams (i.e., the reject and permeate streams) flow countercurrently to one another and that the total pressure is uniform in both the streams.

First, this simple model was applied to the case for separation of air in module 24. Figure 9 shows

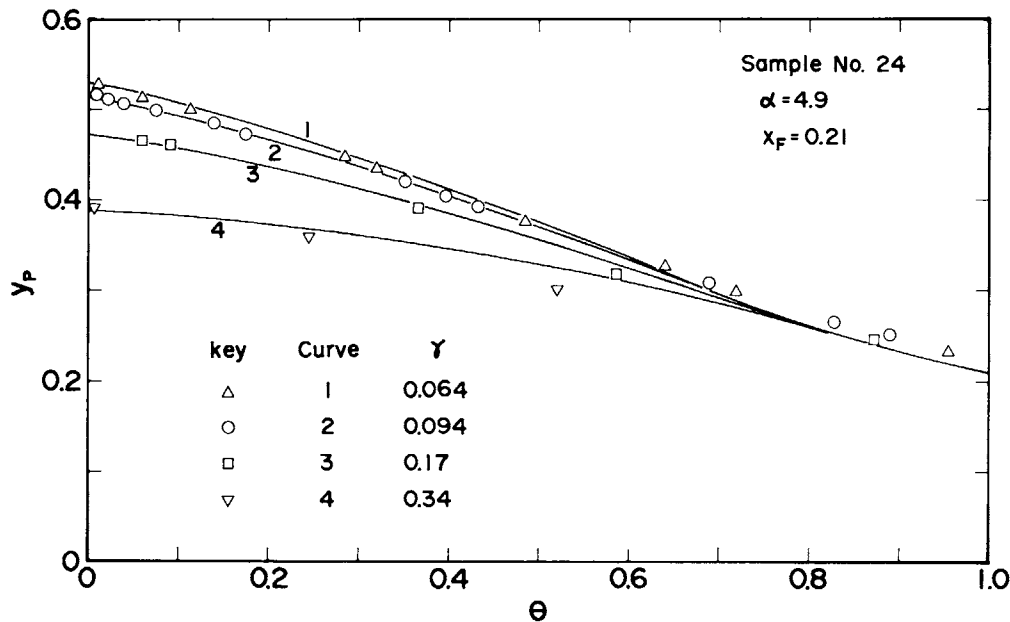


**Figure 9** Relationship between molar fraction of  $O_2$  in the permeate stream and stage cut at four levels of feed-side pressures in the permeation of air at  $30^\circ\text{C}$ . Solid curves refer to calculated ones.

the experimental results on the relation of the composition of  $O_2$  in the permeate stream to the stage cut at four levels of upstream pressure. The upstream pressure ( $p_2$ ) ranges from 0.197 to 1.47 MPa, i.e.,  $\gamma (= p_1/p_2)$  from 0.34 to 0.064. Here, the ideal separation factor of  $O_2$  relative to  $N_2$  was replaced with 4.9, though it was calculated to be 5.5 from measurements of permeation rate coefficients for these two gases as shown in Figure 2. It is apparent that reasonable agreement between observed and calculated compositions of  $O_2$  in the permeate stream has been achieved for the whole range of the stage cut.

Next, helium enrichment was simulated. For the sake of convenience, consider the separation of a binary mixture of He and air (regarded as one component) instead of a ternary mixture of He,  $O_2$ , and  $N_2$ . Accordingly, the ideal separation factor for He that was required for numerical calculation in terms of the present simple model was taken to be an adjustable parameter. The full curves in Figures 7 and 8 represent the computed relationships between the mole fraction of He in the permeate stream and the stage cut. The values of the ideal separation factor employed for numerical calculation are listed in the same figures. It is found that at high stage cuts the simple model overestimates the molar fraction of He in the permeate stream. This may be due mainly to back-mixing in the reject stream (i.e., shell side).

With an increasing stage cut, the variation of concentration of He along the flow direction in the shell side becomes great and, hence, the influence of back-mixing on the profile of He concentration also becomes great.

## CONCLUSION

The permeation behavior of pure He and separation characteristics of the He-air mixture were examined using asymmetric hollow-fiber-type membrane modules of cellulose triacetate. The permeation rate coefficients for He slightly increased with increasing upstream pressure, whereas those for  $O_2$  and  $N_2$  were independent of upstream pressure. The observed permeation rate coefficients for He agreed fairly well with those calculated on the basis of the assumption that the permeate flow inside the fiber is governed by the Hagen-Poiseuille equation. In the single-stage hollow-fiber module used, the molar fraction of He in the permeate stream was increased to 0.99 and 0.999 at stage cuts lower than 0.3, when the molar fraction in the feed stream was 0.90 and 0.99, respectively. The mole fractions of He in the permeate stream were numerically evaluated by a countercurrent plug flow model.

## NOMENCLATURE

$A_t$  total membrane area in the module,  $\text{cm}^2$   
 $D_i$  hollow fiber inside diameter, m or mm  
 $D_0$  hollow fiber outside diameter, m or mm  
 $J_s$  steady-state permeation flux,  $\text{cm}^3$  (STP)/( $\text{cm}^2$  s) or  $\text{mol}/(\text{m}^2 \text{ s})$   
 $l$  hollow fiber length variable measured from the closed end, m or cm  
 $L_t$  total length of the hollow fiber, m or cm  
 $N_t$  total number of hollow fibers in the module  
 $P$  local permeability coefficient,  $\text{mol m}/(\text{m}^2 \text{ s Pa})$ ,  $\text{cm}^3$  (STP)  $\text{cm}/(\text{cm}^2 \text{ s atm})$ , or  $\text{cm}^3$  (STP)  $\text{cm}/(\text{cm}^2 \text{ s cmHg})$   
 $\bar{P}$  mean permeability coefficient,  $\text{mol m}/(\text{m}^2 \text{ s Pa})$ ,  $\text{cm}^3$  (STP)  $\text{cm}/(\text{cm}^2 \text{ s atm})$ , or  $\text{cm}^3$  (STP)  $\text{cm}/(\text{cm}^2 \text{ s cmHg})$   
 $p$  pressure, Pa or atm  
 $p_0$  permeate-side pressure at the closed end, Pa or atm  
 $p_1$  permeate outlet pressure, Pa or atm  
 $p_2$  feed-side pressure, Pa or atm  
 $R$  gas constant,  $\text{J}/(\text{mol K})$   
 $T$  temperature, K  
 $V$  local permeate flow rate per a hollow fiber,  $\text{mol/s}$   
 $v_t$  permeate flow rate at fiber opening per a hollow fiber,  $\text{mol/s}$   
 $x_F$  feed concentration in molar fraction  
 $y_P$  permeate concentration in molar fraction

## Greek Symbols

$\alpha$  ideal separation factor  
 $\alpha'$  separation factor defined by the ratio of permeability for He at 10 atm to permeability for  $\text{O}_2$   
 $\gamma$  ratio of permeate pressure to feed pressure =  $p_1/p_2$   
 $\delta$  effective thickness of the skin layer of asymmetric membrane, cm or m  
 $\Delta p = p_2 - p_1$ , atm  
 $\theta$  stage cut defined as the ratio of permeate flow rate to feed flow rate  
 $\kappa = \bar{P}/\delta$ , permeation rate coefficient,  $\text{mol}/(\text{m}^2 \text{ s Pa})$ ,  $\text{cm}^3$  (STP)/( $\text{cm}^2 \text{ s atm})$ , or  $\text{cm}^3$  (STP)/( $\text{cm}^2 \text{ s cmHg})$   
 $\mu$  viscosity of a gas mixture, Pa s

## REFERENCES

1. S. T. Hwang and K. Kammermeyer, *Membranes in Separation*, Wiley-Interscience, New York, 1975.
2. M. Sidhoum, A. Sengupta, and K. K. Sirkar, *AIChE J.*, **34**, 417 (1988).
3. C. Y. Pan, *AIChE J.*, **29**, 545 (1983).
4. E. Sada, H. Kumazawa, and P. Xu, *J. Appl. Polym. Sci.*, **35**, 1497 (1988).

Received November 3, 1993

Accepted January 26, 1994